Biomedical Science and Engineering, 2016, Vol. 4, No. 1, 23-30
Available online at http://pubs.sciepub.com/bse/4/1/3

DOI:10.12691/bse-4-1-3

Fluorescence Correlation Analysis for Diagnosis Based on Molecular Dynamics

Yasutomo Nomura*

Department of Systems Life Engineering, Maebashi Institute of Technology, Kamisadori, Maebashi, Japan
*Corresponding author: ynomura@maebashi-it.ac.jp

Abstract Fluorescence correlation spectroscopy is a powerful method in clinical laboratory where a lot of samples of patients will be determined because it enables to measure concentration and molecular weight of tested molecules without any physical separation steps. Nevertheless it may not yet be used as widely as one expected. The reason is that it is likely to be difficult for many users to understand the theoretical background. In this method, the users measured intensity fluctuation of fluorescence resulted from the molecules entering and exiting tiny volume element, namely Brownian motion in solution. Using the time series data of fluorescence intensity, the autocorrelation function was calculated. When the function was fit to the analytical model derived from diffusion theory, concentration and molecular weight of fluorophores were obtained. This minireview described the theoretical background of Brownian motion, physical meaning of the correlation analysis, and its usage properly dependent on samples from homogeneous solution to inhomogeneous cell. Furthermore the recent advances are also outlined.

Keywords: *fluorescence correlation spectroscopy, Brownian motion, diffusion theory, diagnosis, clinical laboratory*

Cite This Article: Yasutomo Nomura, "Fluorescence Correlation Analysis for Diagnosis Based on Molecular Dynamics." *Biomedical Science and Engineering*, vol. 4, no. 1 (2016): 23-30. doi: 10.12691/bse-4-1-3.

1. Introduction

Growth in medical expenses in many countries becomes a great burden for the budget [1,2]. The appropriate diagnosis will help to discover diseases in an early stage, which leads to a reduction in medical cost. Furthermore, it would be indispensable to detect a trace amount of diagnostic markers because of the physical and economic load of patients. The methods used often for diagnosis are optical measurements. Especially, researches pay attention to fluorescence that has high sensitivity [3]. Fluorescence measurements were classified into static and dynamic intensity measurement. The former was to evaluate the average intensity alone. In contrast, the later was to determine the average of fluorescence intensity as well as the fluctuation with temporal information, which was able to evaluate dynamic property of the marker.

The temperature in the clinical laboratory is always around 23°C. Both temperatures in cell culture and in vivo are 37°C. These temperatures are resulted in thermal motion of water molecules and Brownian motion of tested marker molecules which is dependent on the molecular weight [4,5,6]. When fluorescent markers in the diluted solution were observed using confocal system, the fluorescence fluctuated because the only a few Brownian particles entering the tiny volume element emitted photons [7]. Briefly, in fluorescence correlation spectroscopy, time-series data on fluorescence fluctuation was subjected to correlation analysis. When the correlation function was fit to the analytical model derived from a simple diffusion equation, we were able to evaluate the properties such as molecular weight and number of fluorescent markers sensitively [8,9,10].

There were several diagnostic methods based on correlation analysis of fluorescence. In fluorescence autocorrelation spectroscopy, FCS, diffusion coefficient and molecular number of the marker with a single fluorescence spectrum was obtained [11,12]. The binding of molecules with different fluorescence spectra was evaluated by synchronized fluctuation in fluorescence cross-correlation spectroscopy, FCCS [13,14]. In addition to the time series data in a fixed volume element, we were able to correlate and analyze the temporal image series obtained from laser scanning confocal microscope (LSM) that was used in many laboratories [15,16]. Image correlation spectroscopy, ICS, was appropriate to determine the dynamic properties of fluorescent molecule within a living cell. Although there have been many reports on the diagnostic method using fluorescence correlation analysis, the development is enlivened by recent remarkable progress of quantum dots [17,18]. In this review, theoretical background of fluorescence correlation analysis is described, the the recent and efficient applications are outlined.

2. Theoretical Background

2.1. Brownian Motion

When a mass of tiny particles is put into water, each particle starts to move separately and disperses over time. As sufficient time goes by, the particle concentration

becomes constant macroscopically in any position. At that time the particles keep to move randomly under a microscope. Thus Brownian motion that never stops under ambient temperature is behind a diffusion phenomenon dependent on concentration gradient [4]. As shown in Figure 1, Brownian motion can be simulated by Monte Carlo model using random number. In this simulation, a particle that was at the origin of coordinates at time 0 moved randomly to new position, namely from the fourth to the first and then the second quadrant. In addition to the Monte Carlo simulation, the concentration of Brownian particles in any time and any position can be also described by diffusion equation.

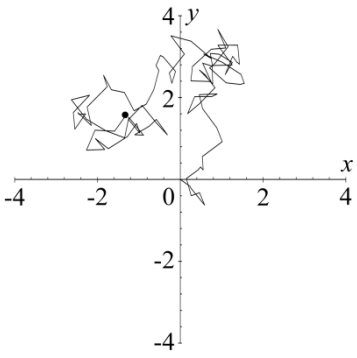

Figure 1. Typical Monte carlo simulation of random walk due to Brownian particle. In this simulation, the renewal of the position is repeated by adding random numbers generated between -0.5 and 0.5 to x and y coordinates. Here a Brownian particle moved from the origin of coordinates to the fourth, the first and the second quadrant

When concentration of molecules is inhomogeneous spatially, molecules diffuse to be homogenous. The larger concentration gradient is, the more molecules move to a sparse area. Thus because the flux of molecules *J*, number of molecules that cross unit cross-sectional area per unit time, is proportional to spatial concentration gradient, we have

$$J = -D\frac{\partial c}{\partial x}, \tag{1}$$

where the concentration and diffusion coefficient are *c* and *D*, respectively. Because the molecules move from a dense area to sparse, the proportional constant has a negative sign. Considering the flux of molecules, we can put concentration changes per unit time as differences between number of molecules entering and that exiting infinite small space. Thus we have

$$\frac{\partial c}{\partial t} = -\frac{\partial J}{\partial x}. \tag{2}$$

Substituting Eq.1 for Eq.2, Eq.3 can be written

$$\frac{\partial c}{\partial t} = D\frac{\partial^2 c}{\partial x^2}. \tag{3}$$

Eq.3 is diffusion equation described as a linear partial differential equation of second order that can be solved analytically. Using Dirac delta distribution as initial conditions, the solution of the equation is described as

$$c(x,t) = \frac{1}{\sqrt{4\pi Dt}}\exp\left(-\frac{x^2}{4Dt}\right). \tag{4}$$

Diffusion coefficient *D* means how far the molecules diffuse per unit time. According to Einstein-Stokes equation, *D* is defined as

$$D = \frac{k_B T}{6\pi\eta r}, \tag{5}$$

where k_B, T, η, r are Boltzmann constant, absolute temperature, viscosity of medium, radius of molecule, respectively. Thus, the molecules diffuse slowly when the molecular radius increases.

2.2. Confocal System

Brownian motion of fluorescently tested biomolecules was able to be measured using confocal system which converted its motion to fluorescence fluctuation [19]. As shown in Figure 2, tiny volume element of the observed area was formed in the optical system which consisted of laser as a point source of light and pinhole aperture in front of a detector. The light of point source excited fluorescent molecules within the volume element and pinhole aperture restricted fluorescence exterior to the area.

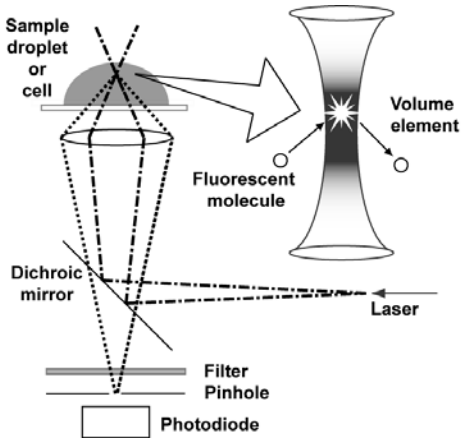

Figure 2. Volume element in confocal system. Through a dichroic mirror, laser light of a point source excites fluorescent molecules within sample droplet or cell if they are within volume element. Fluorescence from volume element alone is detected by photodiodes behind pinhole

When the fluorescent molecules due to Brownian motion enter the volume element, they emit photons and the exiting molecules stop to emit. Therefore, fluorescence measured from the volume element fluctuates over time. The fluorescence intensity at time *t*, $I(t)$, consists of the average $\langle I \rangle$ and the deviation at that time $\delta I(t)$. Thus we have

$$I(t) = \langle I \rangle + \delta I(t). \tag{6}$$

Patterns of fluorescence fluctuation differ dependent on concentration and molecular weight of fluorescent molecules. As shown in Figure 3 A and B, relative ranges of the deviation to the average intensity become narrow when the number of molecular within the volume element increases. Furthermore, when molecular weight of fluorescent molecules increases, slow Brownian motion gives the decrease in frequency of fluorescence fluctuation (Figure 3A and C). Therefore, time series data of fluorescence fluctuation contain information on number and molecular weight of fluorescent molecules (Figure 3D).

3. Autocorrelation Analysis of Fluorescence Fluctuation

The time series data of fluorescence fluctuation were correlated to characterize the fluorescent molecules. There are two correlation analyses of autocorrelation and cross-correlation. The autocorrelation function is given by the ensemble average of the product of fluorescence intensity at time t and that after a delay time τ (Figure 4). The function is generally normalized by the square of an average intensity in FCS and we have

$$G(\tau)=\frac{\langle I(t)\cdot I(t+\tau)\rangle}{\langle I\rangle^2}. \tag{7}$$

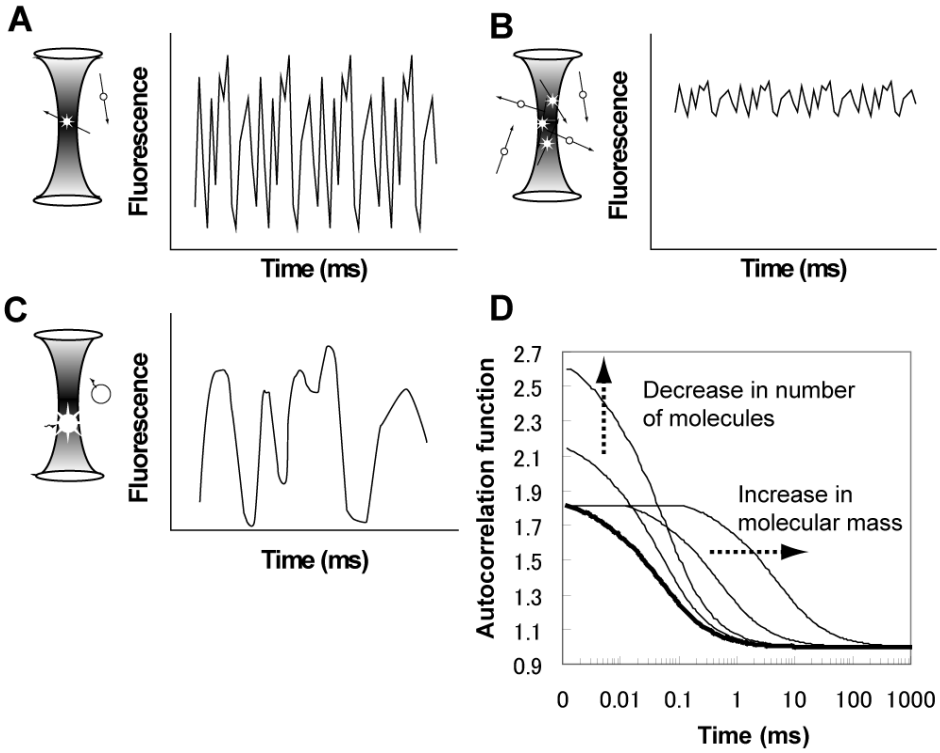

Figure 3. Fluorescence fluctuation and fluorescence autocorrelation curves dependent on number of molecules and molecular weight. (A) Fluorescence due to only a few molecules fluctuates largely. (B) When fluorescent molecules increase, the relative width of deviation to an average intensity becomes narrow. (C) Fluorescence of large molecules fluctuates slowly. (D) Correlation amplitude increases when the number of molecules decreases. When large molecules stay in the volume element for a longer time, namely they diffuse slowly, high amplitude lasts and autocorrelation function is shifted to the right

Substituting Eq.6 for Eq.7, Eq.8 can be written as

$$G(\tau)=1+\frac{\langle \delta I(t)\cdot \delta I(t+\tau)\rangle}{\langle I\rangle^2}. \tag{8}$$

When τ is very short, the sign of the product of two deviation of Eq.8 becomes plus because most of the deviations have the same sign. In the case of long τ, plus and minus in the sign distribute randomly and the second term in the right side of Eq.8 is 0. Therefore, the autocorrelation function has an asymptote of 1 as shown in Figure 3 D.

The autocorrelation function obtained experimentally is assumed to be resulted from N molecules within the volume element. Here, fluorescent molecules consist of a single component. The i-th fluorescent molecule at time t is located to the position $r_i(t)$. Because intensity of fluorescence is proportional to that of excitation, each molecule emits the fluorescence according to the intensity distribution function of excitation $\Phi(r)$. Because fluorescence intensity at time t, $I(t)$, can be written as a sum of fluorescence from each molecule, we have

$$I(t)=\sum_{i=1}^{N}\langle I^s\rangle\cdot\Phi(r_i(t)), \tag{9}$$

where $\langle I^s\rangle$ is the average of fluorescence intensity of a single molecule. Substituting Eq.9 for Eq.7, Eq.10 can be obtained as

$$G(\tau)=\frac{1}{N^2}\left\langle\sum_{i=1}^{N}\Phi(r_i(t))\cdot\sum_{j=1}^{N}\Phi(r_j(t+\tau))\right\rangle. \tag{10}$$

If $i\neq j$, plus and minus in the sign of the product of two deviation of Eq.8 distribute randomly. In other words, signals from two molecules do not correlate independent of τ and thus we have

$$G(\tau)=1. \tag{11}$$

If $i=j$, the autocorrelation function is a sum of that derived from N molecules of the same molecule. Therefore, Eq.10 can be written as

$$G(\tau)=\frac{\langle\Phi(r(t))\cdot\Phi(r(t+\tau))\rangle}{N}. \tag{12}$$

Since fluorescence fluctuation contains the signals of both cases, we obtain the autocorrelation function as a sum of Eq. 11 and Eq.12 by

$$G(\tau)=1+\frac{\langle\Phi(r(t))\cdot\Phi(r(t+\tau))\rangle}{N}. \quad (13)$$

In the second term of right side in Eq.13, the ensemble average can be theoretically calculated using the intensity distribution function and the probability by which Brownian particles diffuse from position r to new position r' during τ, $P(r,r',\tau)$. We can write the equation by

$$G(\tau)=1+\frac{1}{N}\int_{-\infty}^{\infty}\int_{-\infty}^{\infty}\Phi(r)\Phi(r')P(r,r',\tau)drdr'. \quad (14)$$

The intensity distribution function is assumed to be Gaussian function with a peak intensity A because laser of light source is Gaussian beam. Thus we have

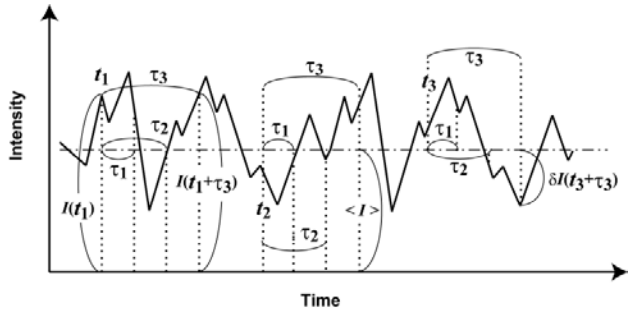

Figure 4. Scheme of time series data of fluorescence intensity. Fluorescence intensity at time t_n $I(t_n)$ and average intensity $\langle I\rangle$ denotes solid line and chain line, respectivey, and the deviation $\delta I(t_n)$ equals to the difference between $I(t_n)$ and $\langle I\rangle$. The autocorrelation function is given by the ensemble average of the product of fluorescence intensity or the deviation at a time and that after a delay time τ

$$\Phi(r)=A\exp\left(-\frac{2r^2}{{\omega_0}^2}\right), \quad (15)$$

where ω_0 is Gaussian beam radius. Substituting Eq.4 and Eq. 15 for Eq.14, and when the integral part is solved as for x, the equation can be obtained by

$$X=A^2\sqrt{\frac{\pi{\omega_0}^2}{4}}\cdot\frac{1}{\sqrt{4D\tau/{\omega_0}^2+1}}. \quad (16)$$

Diffusion time τ_D is assumed as time when Brownian particles with diffusion coefficient D traverses the volume element and D is defined by

$$D=\frac{{\omega_0}^2}{4\tau_D}, \quad (17)$$

When the peak of intensity distribution function is $A=\sqrt[4]{\frac{4}{\pi\omega_0}}$, *Eq*.17 can be written concisely by

$$X=\frac{1}{\sqrt{1+\tau/\tau_D}}. \quad (18)$$

When the integral part is solved as for y, the equation can be similarly obtained. As for z, the equation can be obtained using structure parameter $s=\omega_0/\omega_z$ by

$$Z=\frac{1}{\sqrt{1+s^2\tau/\tau_D}}, \quad (19)$$

where ω_z is the axial half axis of volume element. Using Eq.18~19, Eq.14 can be summarized by

$$G(\tau)=1+\frac{1}{N(1+\tau/\tau_D)\sqrt{1+s^2\tau/\tau_D}}. \quad (20)$$

In Eq.20, the analytical model means that N molecules with fluorescence stay in volume element during τ_D. Thus the amplitude of the autocorrelation function in Figure 3D decreases when N increases. Furthermore, the autocorrelation function shifts to the right when τ_D increases. If data interpretation is consistent with the model, the autocorrelation function obtained experimentally can be fit to Eq.20 using a nonlinear least squares algorithm. When structure parameter s as an apparatus constant is previously determined, N and τ_D of Eq.20 are obtained by the fitting.

The simple one component model was described as above. When various applications to wide clinical fields were considered, concentration changes in the specific component in two or multi-component model would be required to be evaluated. The obtained autocorrelation function was fitted by the multi-component model as

$$G(\tau)=1+\frac{1}{N}\sum_i\frac{f_i}{(1+\tau/\tau_i)\sqrt{1+s^2\tau/\tau_i}}, \quad (21)$$

where f_i and τ_i are the are the fraction and diffusion time of component i, respectively. To distinguish the two components in FCS analysis, their diffusion times must differ with factor more than 1.6, which corresponds to the molecular weight ratio of 4 [20]. Fujii *et al*. detected the prion protein with the fragment of anti-prion antibody fluorescently labeled and another antibody bound to the different epitope for weighting successfully [21]. In mitochondrial genome, the DNA damage by active oxygen species and the DNA polymorphism were analyzed by the two component model and the multicomponent model, respectively [9,10].

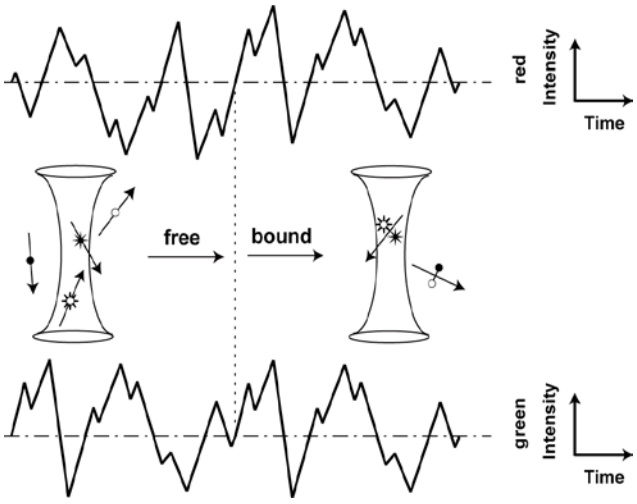

Figure 5. Scheme of fluorescence cross-correlation spectroscopy. Green and red fluorophores behave independently before binding, but each fluorescence fluctuates synchronously when both interact

4. Cross-correlation Analysis

In Brownian motion of two species of molecules with different emission wavelengths, e.g., green and red, the fluorescence intensity of each fluorophore in a volume element fluctuates over time independently. When one color molecule is bound with another, two color fluctuations are synchronized as shown in Figure 5. This phenomena can be analyzed by FCCS [13,22].

When two color fluorescence of green and red are I_g and I_r, respectively, the cross-correlation function $G_c(\tau)$ can be calculated from time series data of the fluorescence fluctuations as similar with Eq.7 by

$$G_c(\tau)=\frac{\langle I_g(t)\cdot I_r(t+\tau)\rangle}{\langle I_g\rangle\langle I_r\rangle}. \quad (22)$$

In the simple analytical model, there are two assumptions; two intensity distribution functions of lasers with different excitation wavelengths are identical to $\Phi(r)$ and two volume elements overlay completely. When the average number of green fluorescence molecules and that of red fluorescence molecules within the volume element are N_g and N_r, respectively, each color fluorescence is a sum of fluorescence due to individual molecules. We put these intensities by

$$I_g(t)=\sum_{i=1}^{N_g}\langle I_g^s\rangle\cdot\Phi(r_i(t)), \quad (23)$$

$$I_r(t+\tau)=\sum_{j=1}^{N_r}\langle I_r^s\rangle\cdot\Phi(r_j(t+\tau)), \quad (24)$$

where $\langle I^s{}_g\rangle$ and $\langle I^s{}_r\rangle$ are the average of fluorescence intensity of a single molecule for green and red, respectively. Substituting Eq.23 and 24 for Eq.22, Eq.25 can be written by

$$G_c(\tau)=\frac{\left\langle\left(\sum_{i=1}^{N_g}\Phi(r_i(t))\right)\cdot\left(\sum_{j=1}^{N_r}\Phi(r_j(t+\tau))\right)\right\rangle}{N_g\cdot N_r}. \quad (25)$$

When each fluorescence fluctuates independently, the sign of the product of two deviation from each average intensity distributes randomly as similar to Eq.11. Thus we obtain the cross correlation by

$$G_c(\tau)=1. \quad (26)$$

Synchronized fluctuations of different fluorescence are only resulted from the number of bound molecules N_{gr}. Because the cross-correlation function is given by a sum of the same ensemble average of the product of fluorescence intensity, we have

$$G_c(\tau)=\frac{N_{gr}\langle\Phi(r(t))\cdot\Phi(r(t+\tau))\rangle}{N_g\cdot N_r}. \quad (27)$$

Since fluorescence fluctuation contains the signals of both cases, the cross-correlation function should be a sum of Eq. 26 and Eq.27, we obtain

$$G_c(\tau)=1+\frac{N_{gr}\langle\Phi(r(t))\cdot\Phi(r(t+\tau))\rangle}{N_g\cdot N_r}. \quad (28)$$

In the analytical model that N_{gr} of bound molecules with two color fluorescence stay in volume element during τ_D, the cross-correlation function obtained experimentally can be fit to

$$G_c(\tau)=1+\frac{N_{gr}}{N_g\cdot N_r(1+\tau/\tau_D)\sqrt{1+s^2\tau/\tau_D}}. \quad (29)$$

When $\tau=0$, the correlation amplitude contains the number of molecules, namely N_{gr}, N_g, N_r, thus we obtain

$$G_c(0)=1+\frac{N_{gr}}{N_g\cdot N_r}. \quad (30)$$

In addition to the cross-correlation analysis of green and red fluorescence, the autocorrelation analysis of each fluorescence gives $G_g(0)$ and $G_r(0)$. Using these values, the number of bound molecules can be obtained from

$$N_{gr}=\frac{G_c(0)-1}{[G_g(0)-1][G_r(0)-1]}. \quad (31)$$

This method was used for determination of molecular interaction as well as detection of trace amount of tested molecules successfully. For bovine spongiform encephalopathy diagnosis, Fujii *et al*. detected prion protein sensitively much more than FCS [21]. One of the difficulties in the method is that the volume element formed by fluorescence of green matches that of red exactly. If there is a positional shift of each volume element, no cross-correlation signals of bound molecules are observed. Researchers developed quantum dots with red fluorescence and found that the interesting excitation spectra covered entire visible region [17]. It was possible that the blue light of a single laser excited dye molecules with green fluorescence as well as the quantum dots with red fluorescence. Although the quantum dots may be suitable for being used for homogeneous solution such as hemolysate, it should be paid to attention when biomolecules within living cells were labelled by them. It was found that a fluorescent protein had a red emission spectrum where the crosstalk of fluorescence due to another fluorophore was able to be neglected. Using the fluorescent proteins genetically engineered, namely, combining a monomeric version of Keima (emission maxima at 620 nm) with cyan fluorescent protein (505 nm) allowed dual-color FCCS with a single 458-nm laser line and complete separation of the fluorescent protein emissions [23].

5. Image Correlation Spectroscopy

In the case of the homogeneous sample such as a solution, FCS and FCCS give the number of molecules and diffusion time which were independent of the observation area. Image correlation spectroscopy, ICS, is a method similar to FCS but may be more suitable for the inhomogeneous sample such as a living cell [15,24]. In ICS, the average dynamic properties of fluorescent

molecule are analyzed in the region of interest, ROI, of temporal image series observed by a laser scanning microscope which has confocal optics. As shown in Figure 6, when $I(x,y,t)$ is the intensity at pixel (x,y) in ROI of the image recorded at time *t*, and $\langle I(x,y,t)\rangle$ is the average intensity of that image at time *t*, the general expression of image correlation analysis is

$$r(\xi,\eta,\tau)=\frac{\langle \delta I(x,y,t)\cdot \delta I(x+\xi,y+\eta,t+\tau)\rangle}{\langle I(x,y,t)\rangle^2}, \quad (32)$$

where $\delta I(x,y,t)=\langle I(x,y,t)\rangle - I(x,y,t)$. ξ and η are spatial lag variables corresponding to pixel shifts of the image relative to itself in the *x* and *y* directions. Briefly, in ICS, the spatial correlation function is firstly calculated and then the number of particle is obtained. Next, using the value, when the temporal correlation function is fitted to an analytical model derived from diffusion theory, diffusion coefficient is calculated.

A spatial autocorrelation function is calculated from the intensities recorded in the pixels of ROI of individual images (Figure 6A). To obtain point spread function of the microscope, fluorescence fluctuations over plane of each image are correlated from Eq. 32 as $\tau=0$ and we have

$$r(\xi,\eta,0)=\frac{\langle \delta I(x,y,t)\cdot \delta I(x+\xi,y+\eta,t)\rangle}{\langle I(x,y,t)\rangle^2}. \quad (33)$$

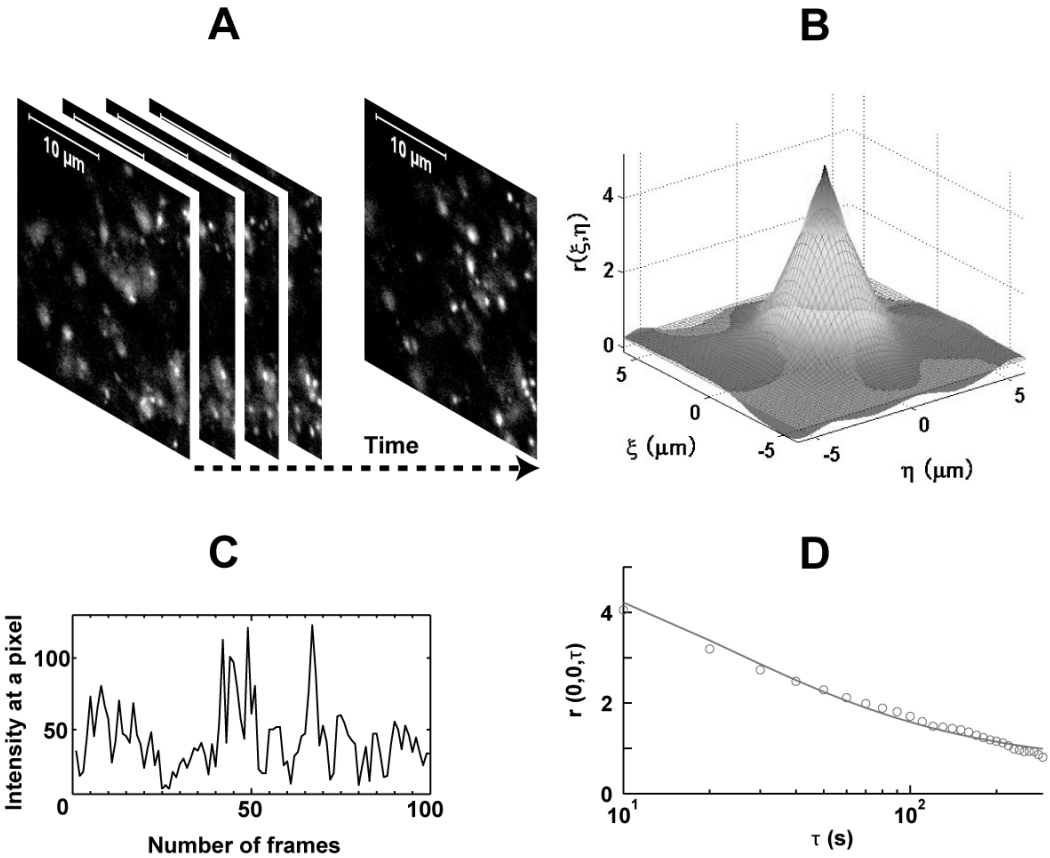

Figure 6. Image correlation spectroscopy [25]. (A) Several frames of time image series. (B) Spatial ICS to obtain the point spread function of LSM (see text). The raw spatial autocorrelation function of the 1st frame of the image series is denoted by the grey surface, and the fitted 2D Gaussian function is denoted by the grey mesh. The point spread function, i.e., beam radius of LSM, is obtained by the fitting. (C) Intensity at a pixel fluctuates with number of frames. (D) Temporal ICS to obtain the diffusion time. A temporal image autocorrelation function (open circles) was derived from the time image series. The temporal autocorrelation function was fitted to a simple one component 2D model (solid line) which can be derived from the diffusion equation

As shown in Figure 6B, the correlation function is then fitted to a two dimensional Gaussian using a nonlinear least squares algorithm and we have

$$r(\xi,\eta,0)=g(0,0,0)\cdot\exp\left[-\frac{\xi^2+\eta^2}{{\omega_0}^2}\right]+g_\infty, \quad (34)$$

where $g(0,0,0)$ is the zero-lags amplitude and is inversely proportional to the number of fluorescent particles, and g_∞ is the long-spatial lag offset to account for an incomplete decay of the correlation function. In Eq. 34, a Gaussian function is used because the laser beam has a Gaussian intensity profile. Dynamics of fluorescent particles is calculated from temporal fluctuation of fluorescence intensity in the area (Figure 6C). As shown in Figure 6D, temporal autocorrelation function of an image series as a function of time lag τ is obtained from Eq. 32 when ξ and η = 0 by

$$r(0,0,\tau)=\frac{\langle \delta I(x,y,t)\cdot \delta I(x,y,t+\tau)\rangle}{\langle I(x,y,t)\rangle^2}. \quad (35)$$

Experimentally, τ values are determined by the time between subsequent images in the image series. Depending on the microscope system used, sampling time of image acquisition is usually between 0.03 and 10 s [16].

Here, the autocorrelation function $r(0,0,\tau)$ is fitted to a simple one component in the two dimensional model which can be derived from the diffusion equation similar to Eq.20.

$$r(0,0,\tau) = \frac{g(0,0,0)}{(1+\tau/\tau_D)} + g_\infty, \quad (36)$$

where $g(0,0,0)$ is the zero-lags amplitude dependent on the number of fluorescent particles, and g_∞ is the long-time offset. For confocal excitation, the characteristic diffusion time, τ_D, is related to the diffusion coefficient, D according to Eq.17.

The diffusion coefficient gives information on dynamics as the average value of ROI in inhomogeneous sample. Because the sampling rate of frames was slightly dependent on the diffusion coefficient obtained, the rate should be set to be proper for dynamics of tested molecules. As for the feasibility of diagnoses for mitochondrial disease, authors used ICS to determine diffusion coefficient of mitochondria and mtDNA simultaneously in a living a single cell [25]. Although ICS permitted to evaluate diffusion constant up to approximately 0.1 $\mu m^2/s$ in case of macromolecules such as mtDNA as well as membrane proteins, small molecules or soluble proteins diffuse too quickly to be determined by ICS. Digman *et al*. developed a raster image correlation spectroscopy, RICS, to be able to measure 10 $\mu m^2/s$ of diffusion coefficient using commercially available LSM [26]. In addition to the autocorrelation analysis of the images, the cross-correlation signals were also obtained from the image series dual-labelled [27].

6. Perspectives

There are several noninvasive methods based on light absorption and scattering such as near infrared spectroscopy and laser Doppler flowmetry. In contrast, FCS may be a little weak as a noninvasive method. For examples, few intrinsic fluorophores have the spectra in the near infrared region. Thus, in the diagnosis using the near infrared region, the marker biomolecule must be labelled fluorescently. On the other hand, it is not easy to set the long working distance, because FCS use confocal system. However, FCS permitted applying to the deep tissue when fluorophores were excited by two-photon or multi-photon. The advantage of FCS is that it would detect the trace amount of tested molecules in blood or biopsy sample which the staff of clinical laboratory treat usually, e.g., HbA1c for diagnosis of diabetes (data not shown).

7. Concluding Remarks

Correlation analysis of fluorescence allowed the evaluation of dynamics of tested molecules in homogeneous solution as well as inhomogeneous sample such as living cells. Therefore the method covered the spectrum for diagnosis wider than the previously used methods. In the case of diagnosis of mitochondrial diseases, southern blotting was used previously but the correlation analysis was applied from mtDNA fragment length distribution to mtDNA dynamics [10,16]. Since FCS enabled the evaluation of the tested molecules without any physical separation steps required in immunochemical assay, the number of the user would increase more and more.

Although this method may not be much familiar to most of the user, physical meaning of the results obtained requires to be understood through several reviews including this paper. When the users do so, they would pay attention to the advanced method of FCS. Pozzi *et al*. analyzed the effect of nonhomogeneous and variable flow on the cross-correlation function and showed an application of electron multiplying charge-coupled device-based fluorescence cross-correlation spectroscopy to blood flow in zebrafish embryos in vivo [28]. By coupling the interferometer with the scanning mirrors and by computing the cross-correlation function of fluorescent red blood cells, they enabled to map speed patterns in embryos' vessels. Because dynamics of tested molecules was analyzed successfully in spatial and temporal resolution with high sensitivity, the progress in medical application and biomedical research would be expected. Furthermore, as for the drug after the diagnosis due to the correlation analysis of fluorescence, high throughput screening for specific inhibitors of target protein in the disease was proposed [29].

In this correlation analysis, when only a few fluorophores with high quantum yield were analyzed, the dynamics of tested molecules was evaluated precisely. In laboratory examination, however, the testing sample frequently contains hemoglobin that may absorb fluorescence from tested molecules. Therefore, we plan to determine the effect of absorption due to hemoglobin on the parameters obtained by FCS. Thus, when one promotes the research of FCS, it is important to keep in mind that the method will be applied to the practical diagnosis.

Acknowledgement

This work was financially supported in part by JSPS KAKENHI Grant Number 23500523, Grant-in-Aid for Scientific Research (C) from Japan Society for the Promotion of Science (JSPS).

References

[1] Gourley, G.A., and Duncan, D.V., "Patient satisfaction and quality of life humanistic outcomes," *The American Journal of Managed Care*, 4(5). 746-752. May 1998.

[2] Poley, M.J., "Nutrition and health technology assessment: when two worlds meet," *Frontiers in Pharmacology*, 6. 232. Oct. 2015.

[3] Lakowicz J., Principles of Fluorescence Spectroscopy, Springer, 2006.

[4] Einstein, A., Investigations on the theory of the Brownian movement, Dover Publications, NY, 1956.

[5] Magde, D., Elson, E.L., and Webb, W.W., "Fluorescence correlation spectroscopy. II. An experimental realization," *Biopolymers*, 13(1). 29-61. Jan. 1974.

[6] Weissman, M., Schindler, H., and Feher, G., "Determination of molecular weights by fluctuation spectroscopy: application to DNA," *Proceedings of the National Academy of Sciences of the United States of America*, 73(8). 2776-2780. Aug. 1976.

[7] Eigen, M. and Rigler, R., "Sorting single molecules: application to diagnostics and evolutionary biotechnology," *Proceedings of the National Academy of Sciences of the United States of America*, 91(13). 5740-5747. Jun. 1994.

[8] Kinjo, M. and Rigler, R., "Ultrasensitive hybridization analysis using fluorescence correlation spectroscopy," *Nucleic Acids Research*, 23(10). 1795-1799. May 1995.

[9] Nomura, Y., Fuchigami, H., Kii, H., Feng, Z., Nakamura, T., *et al*., "Detection of oxidative stress-induced mitochondrial DNA damage using fluorescence correlation spectroscopy," *Analytical Biochemistry*, 350(2). 196-201. Mar. 2006.

[10] Nomura, Y., Fuchigami, H., Kii, H., Feng, Z., Nakamura, T., *et al*., "Quantification of size distribution of restriction fragments in mitochondrial genome using fluorescence correlation spectroscopy," *Experimental and Molecular Pathology*, 80(3). 275-278. Jun. 2006.

[11] Nomura, Y. and Kinjo, M., "Real-time monitoring of in vitro transcriptional RNA by using fluorescence correlation spectroscopy," *ChemBioChem*, 5(12). 1701-1703. Dec. 2004.

[12] Nomura, Y., Tanaka, H., Poellinger, L., Higashino, F., and Kinjo, M., "Monitoring of in vitro and in vivo translation of green fluorescent protein and its fusion proteins by fluorescence correlation spectroscopy," *Cytometry*, 44(1). 1-6. May 2001.

[13] Foldes-Papp, Z., Kinjo, M., Tamura, M., Birch-Hirschfeld, E., Demel, U., *et al*., "A new ultrasensitive way to circumvent PCR-based allele distinction: direct probing of unamplified genomic DNA by solution-phase hybridization using two-color fluorescence cross-correlation spectroscopy," *Experimental and Molecular Pathology*, vol. 78(3). 177-189. Jun. 2005.

[14] Sun, F., Mikuni, S., and Kinjo, M., "Monitoring the caspase cascade in single apoptotic cells using a three-color fluorescent protein substrate," *Biochemical and Biophysical Research Communications*, 404(2). 706-710. Jan. 2011.

[15] Kolin, D.L. and Wiseman, P.W., "Advances in image correlation spectroscopy: measuring number densities, aggregation states, and dynamics of fluorescently labeled macromolecules in cells," *Cell Biochemistry and Biophysics*, 49(3). 141-164. Oct. 2007.

[16] Nomura, Y., "Direct quantification of mitochondria and mitochondrial DNA dynamics," *Current Pharmaceutical Biotechnology*, 13(14). 2617-2622. Nov. 2012.

[17] Fujii F. and Kinjo, M., "Detection of antigen protein by using fluorescence cross-correlation spectroscopy and quantum-dot-labeled antibodies," *ChemBioChem*, 8(18). 2199-2203. Dec. 2007.

[18] Klapper, Y., Maffre, P., Shang, L., Ekdahl, K.N., Nilsson, B., *et al*., "Low affinity binding of plasma proteins to lipid-coated quantum dots as observed by in situ fluorescence correlation spectroscopy," *Nanoscale*, 7(22). 9980-9984. Jun. 2015.

[19] Edman, L., Mets, U., and Rigler, R., "Conformational transitions monitored for single molecules in solution," *Proceedings of the National Academy of Sciences of the United States of America*, 93(13). 6710-6715. Jun. 1996.

[20] Meseth, U., Wohland, T., Rigler, R., and Vogel, H., "Resolution of fluorescence correlation measurements," *Biophysical Journal*, 76(3). 1619-1631. Mar. 1999.

[21] Fujii, F., Horiuchi, M., Ueno, M., Sakata, H., Nagao, I., *et al*., "Detection of prion protein immune complex for bovine spongiform encephalopathy diagnosis using fluorescence correlation spectroscopy and fluorescence cross-correlation spectroscopy," *Analytical Biochemistry*, 370(2). 131-141. Nov. 2007.

[22] Schwille, P., Meyer-Almes, F.J., and Rigler, R., "Dual-color fluorescence cross-correlation spectroscopy for multicomponent diffusional analysis in solution," *Biophysical Journal*, 72(4). 1878-1886. Apr. 1997.

[23] Kogure, T., Karasawa, S., Araki, T., Saito, K., Kinjo, M., *et al*., "A fluorescent variant of a protein from the stony coral Montipora facilitates dual-color single-laser fluorescence cross-correlation spectroscopy," *Nature Biotechnology*, 24(5). 577-581. May 2006.

[24] Nomura, Y. and Kinjo, M., "Editorial: Current optical procedures used in cell biology," *Current Pharmaceutical Biotechnology*, 13(14). 2545-2546. Nov. 2012.

[25] Matsuo, T., Nakayama, K., Nishimoto, K., and Nomura, Y., "Image Processing Methods for Quantitative Analysis of Mitochondrial DNA Dynamics," *Biochemistry and Analytical Biochemistry*, S3-001. 2012.

[26] Digman, M.A. and Gratton, E., "Analysis of diffusion and binding in cells using the RICS approach," *Microscopy Research and Technique*, 72(4). 323-332. Apr. 2009.

[27] Wiseman, P.W., Squier, J.A., Ellisman, M.H., and Wilson, K.R., "Two-photon image correlation spectroscopy and image cross-correlation spectroscopy," *Journal of Microscopy*, 200(1). 14-25. Oct. 2000.

[28] Pozzi, P., Sironi, L., D'Alfonso, L., Bouzin, M., Collini, M., *et al*., "Electron multiplying charge-coupled device-based fluorescence cross-correlation spectroscopy for blood velocimetry on zebrafish embryos," *Journal of Biomedical Optics*, 19(6). 067007. Jun. 2014.

[29] Goto, T., Sato, M., Takahashi, E., and Nomura, Y., "Image analysis of colocalization of nuclear DNA and GFP labelled HIF-1alpha in stable transformants," *Current Pharmaceutical Biotechnology*, 13(14). 2547-2550. Nov. 2012.